CHAPTER 6

INSIGHTS INTO GALAXY SIZE GROWTH FROM SEMI-ANALYTIC MODELS

A major challenge facing the field of galaxy evolution lies in reconciling the observed structural evolution of galaxies with theoretical predictions. The discovery of extremely compact high-redshift galaxies in particular has prompted great efforts to understand their inferred size growth, with varying degrees of success. In this paper we investigate the size growth of quiescent galaxies as predicted by semi-analytical models. We analyze several SAMs with different prescriptions for galaxy physics in order to uncover robust predictions. By selecting galaxies in the same way as is done in observations, i.e., using mass-selected samples which are separated into quiescent and starforming subsamples using multi-color cuts, we can make a consistent comparison between models and observations. We find that the models closely match observed changes in the median sizes of quiescent galaxies: $r_{\rm eff} \propto (1+z)^{-1.2}$, with very little difference between models. However, the large size difference between starforming and quiescent galaxies that is found in observations is not reproduced by these models. This points to a serious flaw in either the models or observations. On the whole, rapid galaxy size growth is a generic, robust feature, independent of details concerning gas dissipation or disk instabilities. Instead, it is more strongly driven by the underlying growth of dark matter halos and a few simple prescriptions for galaxy sizes. Quiescent and starforming galaxies grow at very similar rates in the models, which can be explained by the fact that newly quenched galaxies dominate the quiescent population in terms of number density. Although changes in the quiescent population are largely driven by the growth of starforming galaxies, we find that galaxies in SAMs still grow significantly in both mass and size after they quench. This growth is such that quiescent galaxies move onto a tight mass-size relation at high masses, regardless of the redshift at which they quenched. At lower masses ($M_* \lesssim 10^{11} M_\odot$), galaxies interact relatively little and consequently remain relatively untouched throughout their further life. As a result of this, at low stellar masses galaxy size correlates with both quenching epoch and mass-weighted age.

Daniel Szomoru, Simone Weinmann, Marijn Franx

6.1 INTRODUCTION

The issue of galaxy size growth has dominated studies of high-redshift galaxy structure ever since the discovery of very small and massive quenched galaxies at $z > 1.5$ about a decade ago (e.g., Daddi et al. 2005; Trujillo et al. 2006; Toft et al. 2007; van Dokkum et al. 2008). Since the discovery of these extreme objects it has been found that both quenched and starforming galaxies are significantly smaller at high redshift compared to low-redshift galaxies of the same stellar mass (e.g., Trujillo et al. 2006; Williams et al. 2010). This size growth is accompanied by evolution in most other structural and morphological features: e.g., an increase in central concentration and surface density, and reddening of stellar populations (e.g., Williams et al. 2010; Szomoru et al. 2011; Bell et al. 2012). This change in average galaxy properties is smooth and continuous, and quite rapid. Perhaps surprisingly, quiescent galaxies have been found to evolve at least as rapidly as starforming galaxies, despite the fact that they have stopped forming new stars.

A robust median growth trend of $r_{\rm eff} \propto (1+z)^{-1}$ has emerged for quiescent galaxies at fixed stellar mass (e.g., Williams et al. 2010; Damjanov et al. 2011, and references therein). Efforts to understand this trend have mainly focused on growth through minor, gas-poor mergers. Recent simulations have shown that a string of such mergers can transform typical $z = 2$ quiescent galaxies into massive $z = 0$ ellipticals (Naab et al. 2009; Oser et al. 2010; Oser et al. 2012; Oogi & Habe 2013; Bédorf & Portegies Zwart 2013). However, galaxy merger rates from observed pair fractions seem to indicate that minor merging does not occur often enough to drive all of the observed growth (Williams et al. 2011; Newman et al. 2012). Matters are further complicated by the difficulty of linking galaxies observed at different redshifts, and by differences in the criteria used to select galaxy samples.

Thus, although the size growth at fixed mass between $z = 2$ and the present day is quite well-measured, the interpretation of this measurement is not straightforward. One promising possibility lies in the use of semi-analytic models (SAMs). Using these models it is possible to relatively quickly test the effects of different implementations of galaxy physics such as gas dissipation or stellar feedback, and assess the importance of different physical processes for galaxy evolution. Such comparisons between analytic models and observations generally focus on the growth of either pure disks or strongly bulge-dominated galaxies, with the aim of studying specific growth mechanisms such as accretion from halos onto disks or growth due to mergers (e.g., Mo et al. 1999; Somerville et al. 2008; Shankar et al. 2013).

However, separating galaxies by morphology prevents consistent comparisons to observations, since high-redshift galaxies are usually selected based on star formation activity, which can be robustly measured using galaxy colors (Williams et al., 2009). Selecting galaxies by star formation activity not only alters the galaxy samples under consideration, but also changes the physical issue that is addressed. The central question becomes not how disks or bulges form, but rather how galaxies grow while forming stars, and what happens to them once they become inactive. It is clear that simulations must use the same type of galaxy selection as observations in order to answer this question.

In this paper we take a step in that direction by computing the size growth predic-

tions of several SAMs for galaxies which are selected in the same way as observed galaxy samples. Our purpose is not to validate the predictions of SAMs, but rather to use them as toy models for galaxy growth. The models analyzed in this paper are all based on the same dark matter simulation, but differ in the implementation of more detailed physics, such as baryon cooling or the treatment of disk instabilities. The different models thus provide an opportunity to investigate common predictions for a ΛCDM universe, while also highlighting the importance of second-order effects on galaxy structure.

6.2 GALAXY SIZES IN SEMI-ANALYTIC MODELS

We analyze the outputs of two semi-analytic models, both based on the Millenium dark matter simulation (Springel et al., 2005): the Bower et al. (2006) model, which is based on GALFORM (Cole et al., 2000); and the Guo et al. (2011) model, which builds on the models of Springel et al. (2005), Croton et al. (2006) and De Lucia & Blaizot (2007). Output catalogs for these SAMs are available publicly at `http://www.virgo.dur.ac.uk/` and `http://www.mpa-garching.mpg.de/millennium/`.

In terms of structure, galaxies in these SAMs are modeled as a combination of two components: a flat disk and a central bulge. Galaxies initially form as stellar disks, which can then merge or collapse into bulges. Disk growth is calculated following the formalism of Mo et al. (1998). In this formalism diffuse hot halo gas cools into a flat disk under the assumption of angular momentum conservation. Subsequent star formation then transforms this gas disk into a stellar disk, which is assumed to have the same specific angular momentum as the gas disk. Additional material can accrete onto it, changing its mass and angular momentum, and thereby its size.

Bulge formation is implemented in two ways. Firstly, stellar disks can become unstable and fragment if their surface density exceeds some threshold. This threshold is calculated in similar ways in both models, but the subsequent disk fragmentation is treated in different ways. In the Bower et al. (2006) model, when disks become unstable their entire mass is transferred to the central bulge, while Guo et al. (2011) remove matter from the disk until it becomes marginally stable again. This results in a more gradual buildup of bulges and depletion of disks. In either case the resulting bulge size is calculated assuming virial equilibrium.

The second mechanism for bulge growth is through galaxy mergers. There are several possible outcomes for a merger between two galaxies, depending on their mass-ratio. If two equal-mass galaxies merge, all their stellar matter will be transferred into a central bulge. In the case of unequal-mass mergers, all the stellar mass of the lower-mass galaxy is transferred into the massive galaxy's bulge, but the disk of the higher-mass galaxy (if present) is left undisturbed. In both models the presence of gas in the merging galaxies may trigger a central starburst. However, energy loss due to gas dissipation is not implemented in either model; this can result in unrealistically large sizes for intermediate-mass bulge-dominated galaxies (Shankar et al., 2013).

The SAM catalogs provide a disk scalelength and a bulge half-mass radius for each galaxy, as well as total stellar masses and bulge mass fractions. For each galaxy we can thus construct radial stellar mass surface density profiles for the disk and bulge components separately, which we then combine to obtain total stellar mass surface density profiles.

Stellar disks are assumed to be infinitely thin and follow exponential profiles:

$$\Sigma_{*,\mathrm{disk}} = \Sigma_{0,\mathrm{disk}} e^{-r/r_d}, \tag{6.1}$$

where r_d is the disk scalelength. Bulge profiles are calculated by deprojecting the three-dimensional half-mass radius and inserting it into an $n = 4$ Sérsic profile (Sérsic, 1968):

$$\Sigma_{*,\mathrm{bulge}} = \Sigma_{\mathrm{eff,bulge}} e^{[-7.67(r/r_{\mathrm{eff,bulge}})^{-1/4}-1]}. \tag{6.2}$$

The total mass profile can now be straightforwardly obtained by summing the disk and bulge profiles. The half-mass radius of the galaxy is then calculated by integrating the total mass profile.

It is important to note that the effective radii calculated for the galaxies in these SAMs are based on stellar mass distributions, as opposed to the stellar light distributions used in most observations. Szomoru et al. (2013) have shown that the half-mass radii of massive galaxies are on average 25% smaller than their half-light radii, at all redshifts out to $z = 2.5$. The difference between half-mass radius and half-light radius does not seem to depend on redshift or galaxy properties, and therefore the comparison between observed size evolution from half-light radii to size evolution from model half-mass radii should be affected in the same way at all redshifts and should be independent of the sample of galaxies under consideration. Since in this paper we focus on the relative size difference between different redshifts, this constant factor is not a concern.

6.3 GALAXY SELECTION

In order to make a meaningful comparison between the models and observations we use selection criteria commonly used at high redshift. We split the galaxy catalog into quiescent and starforming subsamples using a two-color selection criterium (e.g., Williams et al. 2009). Our color-color cut is calibrated at each redshift using the SFR information in the Guo et al. (2011) catalog. The effectiveness of this color selection is demonstrated in Figure 6.1, where we show the mean SSFR of galaxies in the $u - r$ - $r - z$ plane, at $z = 0$ and $z = 2$. Our selection box, indicated by the dashed lines, is adjusted to optimally separate starforming and quiescent galaxies.

SSFR-based selections and morphological selections are sometimes used interchangeably, since morphology is known to strongly correlate with SSFR at redshifts up to at least $z \sim 2$ (Szomoru et al. 2011; Bell et al. 2012). In the case of simulations and low-redshift observations it is fairly straightforward to obtain detailed morphological information. At high redshift, however, the difficulty of obtaining reliable morphological information has forced observers to distinguish between galaxy populations using SSFR-based quantities.

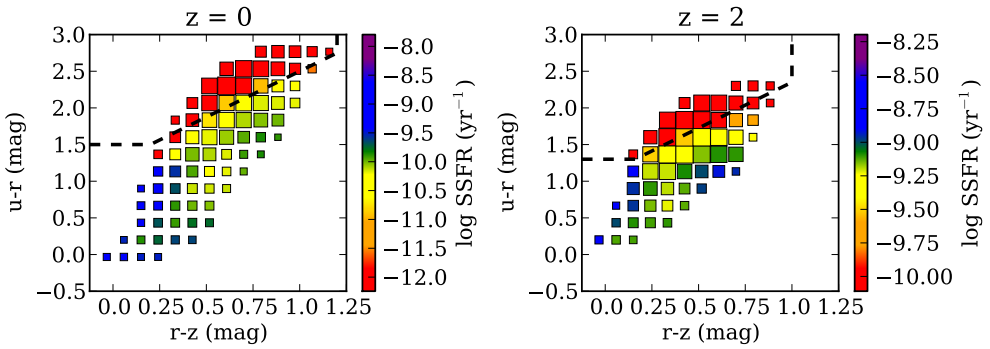

Figure 6.1: $u-r$ versus $r-z$ colors for massive ($10^{10.5} < M_*/M_\odot < 10^{11}$) galaxies from the Guo et al. 2011 SAM catalog, at $z = 0$ and $z = 2$. Color coding indicates SSFR. The dashed lines indicate our quiescent galaxy selection limits. Quiescent galaxies in the models occupy a well-defined region in the urz plane, and can be effectively selected using a two-color selection.

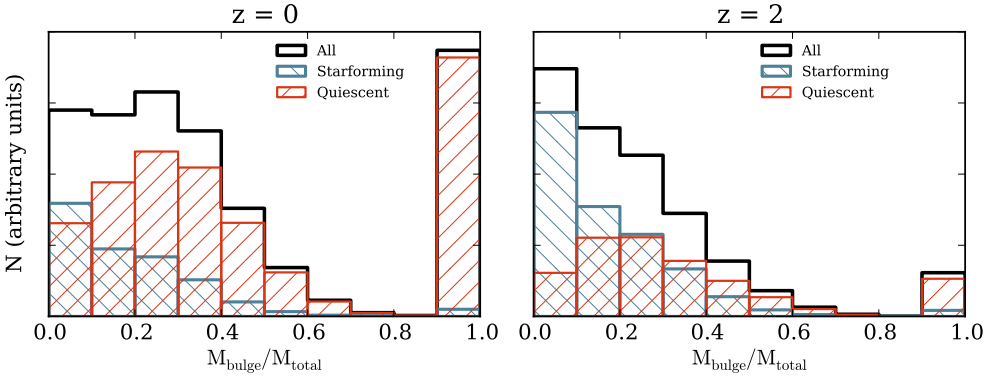

Figure 6.2: The distribution of bulge-to-total mass ratios for quiescent galaxies, starforming galaxies, and all galaxies (red, blue and black histograms, respectively) in the Guo et al. (2011) catalog, with stellar masses $10^{10.5} < M_*/M_\odot < 10^{11}$. The distributions are shown at $z = 0$ and $z = 2$. The distribution of bulge-to-total ratios is very broad, both for quiescent and starforming galaxies. This is the case at all redshifts up to $z = 6$. The median bulge fraction of quiescent galaxies is quite, even at low redshift; at $z = 0$ it is equal to 0.29. It is therefore important to select on star formation activity - not bulge fractions - when comparing model predictions to observations of passive galaxies.

It is important to realize that there is a significant difference between these two selection methods. Although quiescent galaxies are more spheroidal relative to starforming galaxies at all redshifts (i.e., more concentrated, higher Sérsic indices, higher velocity dispersions), they are not necessarily spheroids in an absolute sense. Sérsic indices of quiescent galaxies at $z \sim 2$ are significantly lower than at $z = 0$, and axis ratio distributions suggest that galaxies become more disk-like at high redshift (van der Wel et al. 2011; Chang et al. 2013a;

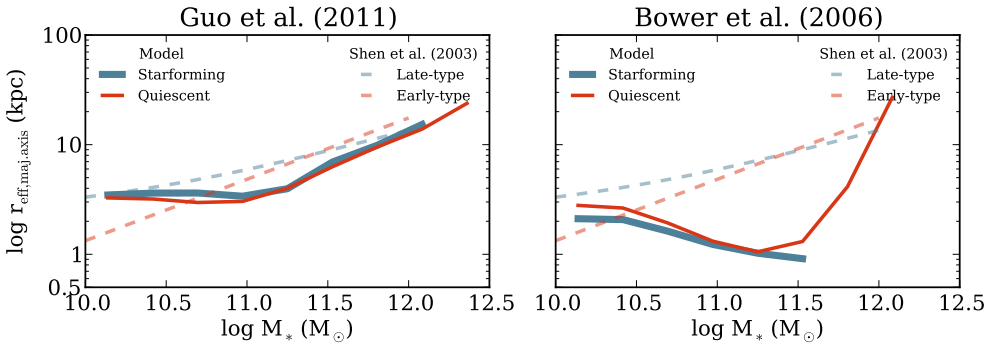

Figure 6.3: Median $z = 0$ mass-size relations for urz-selected quiescent (red) and starforming (blue) galaxies in the Guo et al. (2011) and Bower et al. (2006) models. Observations from Shen et al. (2003) are shown as dashed lines (observed values have been corrected from circularized to major-axis radii). Starforming and quiescent galaxies lie on very similar mass-size relations in both models, which is in agreement with observations in this mass range. The observed slope of the mass-size relation is reasonably well reproduced by the Guo et al. (2011) model, but the Bower et al. (2006) model incorrectly produces a negative slope.

Chang et al. 2013b). Thus, the structure of galaxies changes significantly over this redshift range, which can introduce serious biases into samples which are selected by bulge fraction or concentration.

As an illustration we plot the distribution of bulge-to-total mass ratios for galaxies in the Guo et al. (2011) catalog in Figure 6.2. Quiescent galaxies, starforming galaxies, and the entire galaxy sample are shown in red, blue and black, respectively. It is immediately apparent that in these models a selection based on bulge fraction (or, equivalently, Sérsic index) is not equivalent to a selection based on star formation activity. Cuts of $M_{*,\mathrm{bulge}}/M_{*,\mathrm{total}} > 0.3$ or 0.7 result in either enormous contamination from starforming galaxies (for low $M_{*,\mathrm{bulge}}/M_{*,\mathrm{total}}$ cuts) or exclusion of the majority of quiescent galaxies (for high $M_{*,\mathrm{bulge}}/M_{*,\mathrm{total}}$ cuts). Thus, in order to make a meaningful comparison to high-redshift observations, it is very important to use a star formation-based selection method.

6.4 GALAXY GROWTH

THE MASS-SIZE RELATION AT Z=0

Before addressing the redshift evolution of galaxy sizes it is worthwhile to look at galaxy masses and sizes at $z = 0$, since the models are calibrated to observations at this redshift. In Figure 6.3 we plot the median mass-size relations of starforming and quiescent galaxies in the Guo et al. (2011) and Bower et al. (2006) models as solid lines (left and right panel, respectively). The purple and yellow lines indicate the mass-size relations for late-type and early-type galaxies from Shen et al. (2003). The Shen et al. (2003) values have been corrected from circularized to major-axis radii using median axis ratios for late-type and early-type

galaxies.

The Guo et al. (2011) model performs quite well, producing mass-size relations at $z = 0$ that are in quite close agreement with observations. The overall trend of increasing stellar mass with increasing galaxy sizes is reproduced fairly well, although the slope at low masses ($M_* < 10^{11} M_\odot$) is too low. The size difference between quiescent and starforming galaxies, which is clearly visible in the data at $M_* < 10^{11} M_\odot$, is completely absent in the model. This may be due to the fact that energy loss due to gas dissipation is not implemented in the model's treatment of mergers. Shankar et al. (2013) show that including this process results in smaller sizes for galaxies with $M_* < 10^{11} M_\odot$. However, this does not significantly increase the size difference between starforming and quiescent galaxies (Shankar 2013, private communication).

The Bower et al. (2006) model predicts a mass-size relation that has a negative slope up to $M_* = 10^{11.5} M_\odot$, and has very large scatter at masses above $10^{11} M_\odot$. This is clearly in contradiction with observations. This problem has been the subject of several studies (e.g., González et al. 2009; Shankar et al. 2010a; Shankar et al. 2010b), and is the result of a combination of factors, including the strenght of supernova feedback, the effects of dark matter during galaxy mergers, and the treatment of disk instabilities.

GROWTH AT FIXED MASS

It is clear that SAMs have difficulties in reproducing certain aspects of galaxy structure. The Bower et al. (2006) model, in particular, predicts a relation between stellar mass and size that deviates strongly from observations. As shown by Shankar et al. (2010), the normalization of the Bower et al. (2006) mass-size relation changes with redshift, but the overall shape remains roughly the same. This means that the relative size growth of galaxies might not be strongly affected by issues regarding the shape of the mass-size relation. In Figure 6.4 we compare SAM predictions for galaxy size growth to recent observations by van der Wel et al. (2013, in prep.). We calculate the median effective radii of galaxies with $10^{10.5} < M_*/M_\odot < 10^{11}$, separating them into quiescent and starforming samples as described in Section 6.3 (top panels), and into pure bulges and pure disks (bottom panels). Model values are shown as solid lines, while the data points indicate observations from van der Wel et al. (2013, in prep.). These authors have separated their galaxies using a UVJ color selection, which is comparable to the urz selection we use in this paper. The α values of power-law fits of the form $r_{\rm eff} \propto (1+z)^\alpha$ are provided for each subsample.

The models are remarkably consistent in their predictions; quiescent galaxies grow as $\approx (1+z)^{-1.2}$, well within the range of values measured in observations (e.g., Williams et al. 2010; Damjanov et al. 2011, and many others). The similarity of the predictions of the two models provides important clues regarding the drivers of galaxy size growth; the processes leading to rapid galaxy size growth must be fairly generic and fundamental. The most obvious of these is the dark matter simulation on which the two SAMs are based, which strongly influences the merging behaviour of halos and galaxies. Secondly, the basic prescriptions for galaxy sizes are very similar: gas cooling and subsequent star formation follow roughly the

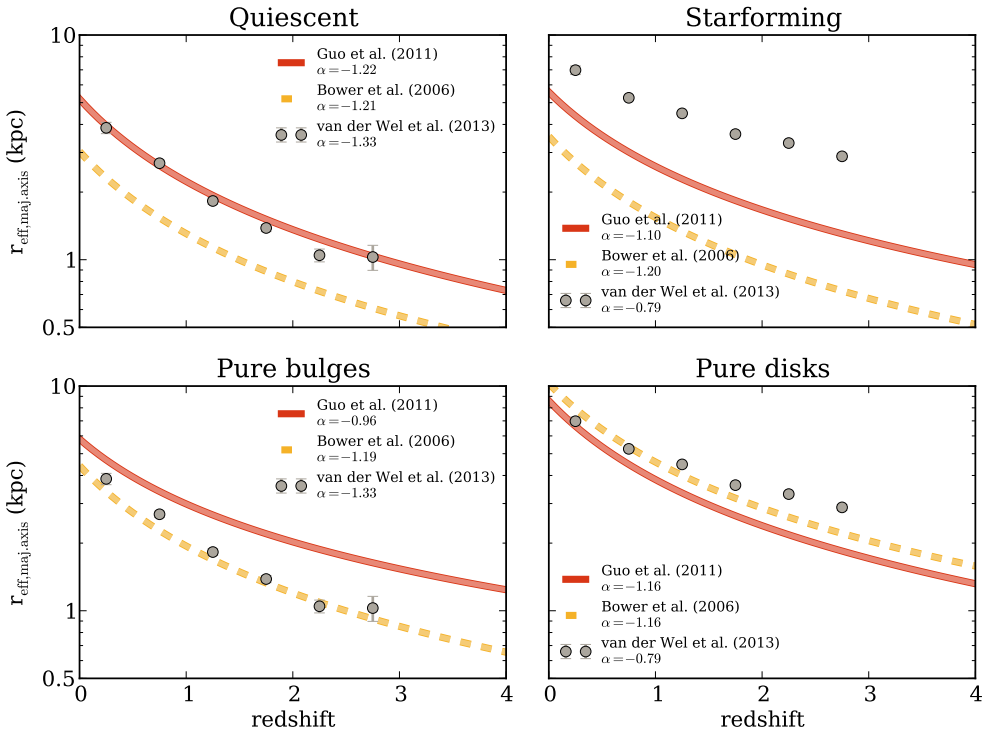

Figure 6.4: Top panels: median size evolution of quiescent and starforming galaxies with stellar masses $10^{10.5} < M_*/M_\odot < 10^{11}$. Red (solid) and yellow (dashed) lines indicate predictions from the Guo et al. (2011) and Bower et al. (2006) models, and observed values from van der Wel et al. 2013 are indicated by the grey data points. Error bars indicate the errors on the median values. Best-fit α parameters from $(1+z)^\alpha$ power law fits are shown. The models robustly predict $\alpha \approx -1.2$ for quiescent galaxies, which is in good agreement with observations. The growth of starforming galaxies is somewhat overestimated in the models, and the sizes of starforming galaxies are on average a factor $\sim 2-4$ too small. Bottom panels: median size evolution of pure bulge and pure disk galaxies in the same mass range. In the Guo et al. (2011) model bulges grow more slowly than quiescent galaxies. In the Bower et al. (2006) model there is very little difference, possibly due to the more rapid action of disk instabilities in this SAM. Pure disk galaxies grow at a rate that is very close to that of starforming galaxies.

same formalism, and the calculation of bulge sizes is based on the same virial arguments. However, disk rotation velocities are calculated in slightly different ways, and the Guo et al. (2011) model treats gas disks and stellar disks separately. Furthermore, disk instabilities act on very different timescales in the two models. As pointed out in Section 6.4, these differences have considerable consequences for observables such as the slope and scatter of the mass-size relation, as wel as the absolute sizes of galaxies, but they do not seem to strongly affect zeroth order galaxy growth.

Both models predict that starforming galaxies grow at a rate that is very similar to that of quiescent galaxies: in the models starforming galaxies grow as $\approx (1+z)^{-1.15}$, which is

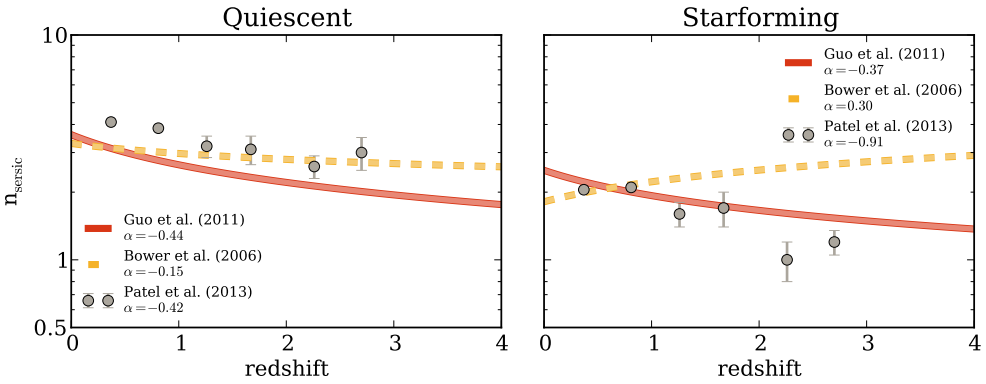

Figure 6.5: Evolution in the mean Sérsic index of galaxies with stellar masses $10^{10.5} < M_*/M_\odot < 10^{12}$. Red (solid) and yellow (dashed) lines indicate predictions from the Guo et al. (2011) and Bower et al. (2006) models, and observed values from Patel et al. (2013) are indicated by the grey data points. Error bars indicate the errors on the median values. Best-fit α parameters from $(1+z)^\alpha$ power law fits are shown. The Guo et al. (2011) model performs very well, predicting Sérsic indices that are very close to observations both in terms of their absolute value and their relative increase with time. The Bower et al. (2006) model correctly predicts the increase in Sérsic index for quiescent galaxies, but does not match the observations for starforming galaxies.

consistent with observations (e.g., Dahlen et al. 2007; Nagy et al. 2011; Mosleh et al. 2012;). In principle there is no reason that these two types of galaxies should grow at similar rates, since the processes that contribute to their build-up are quite different. However, the number density of quiescent galaxies increases by almost an order of magnitude from $z = 2$ to $z = 0$, which means that the quiescent population is always dominated by recently quenched galaxies (e.g., van der Wel et al. 2009; Carollo et al. 2013). Even if galaxies completely stop growing after they quench, the quiescent population as a whole will still grow in size, simply because it is fed with ever-larger starforming galaxies. The degree to which this mechanism dominates is dependent on the size difference between starforming and quiescent galaxies. Figure 6.4 shows that this difference is too small in the models, which may point to a problem in the treatment of the structural transformation that accompanies quenching.

We illustrate the changes in galaxy morphology in Figure 6.5, where we show the change in the mean Sérsic index of quiescent and starforming galaxies. The models are indicated by red (solid) and yellow (dashed) lines, and observations from Patel et al. (2013) are shown as grey datapoints. The model Sérsic indices have been calculated by fitting Sérsic profiles to the 1-D surface density profiles of all the galaxies. Observations show that galaxy Sérsic indices increase quite strongly with time, both for starforming and quiescent galaxies. The Guo et al. (2011) model predicts a rate of increase in the Sérsic indices of quiescent galaxies that is remarkably close to the observations, but underpredicts the change for starforming galaxies. Similarly, the Bower et al. (2006) model performs reasonably well for quiescent galaxies, but very poorly for starforming galaxies. In both models Sérsic indices tend to be low compared to observations; this is most likely simply due to the fact that in

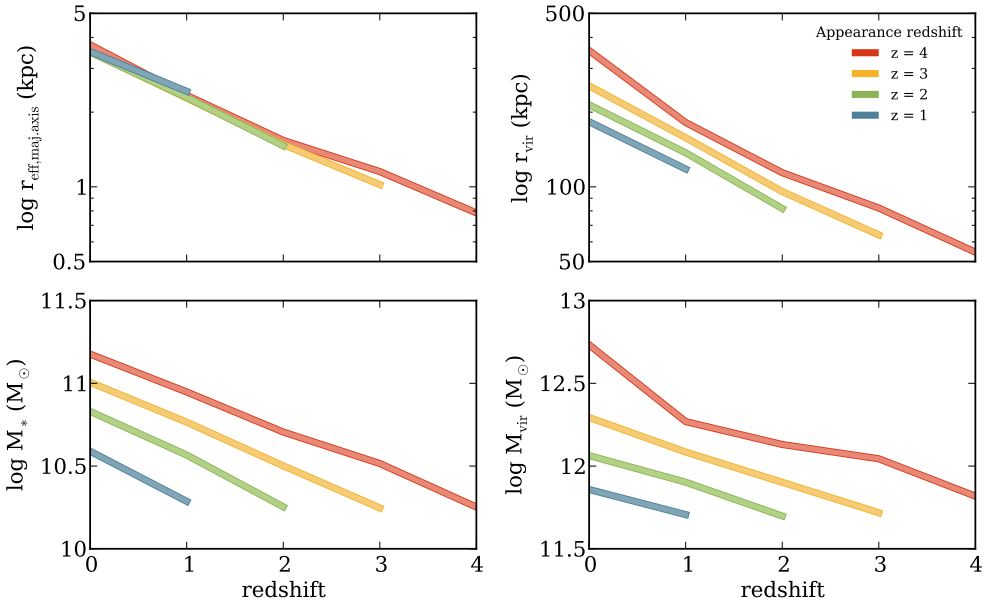

Figure 6.6: Growth in median size, virial radius, stellar mass, and virial mass for starforming galaxies, measured by tracing the descendants of $10^{10} M_{\odot}$ galaxies down to low redshift. Each color corresponds to galaxies which crossed the $10^{10} M_{\odot}$ mass threshold at different redshifts. For clarity, galaxies which quench before $z = 0$ are not shown. Galaxy sizes evolve at almost the same rate as the virial radii of their parent halos: $r_{\rm eff} \propto (1+z)^{-1.2}$, and $r_{\rm vir} \propto (1+z)^{-1.3}$. Stellar masses increase slightly faster than virial masses: $M_* \propto (1+z)^{-1.7}$, and $M_{\rm vir} \propto (1+z)^{-1.2}$.

the models the maximum Sérsic index is $n = 4$ (for a pure bulge), while observed values can be much higher.

THE GROWTH OF STARFORMING GALAXIES

Newly quenched galaxies make up the bulk of the quiescent population; understanding changes in the population of quiescent galaxies therefore becomes a matter of understanding the growth of starforming galaxies. A very naive expectation is that the sizes of stellar disks scale as the virial radii of their parent halos. We investigate this simple assumption by tracking the growth of starforming galaxies. We select populations of starforming galaxies with stellar masses of $10^{10} M_{\odot}$ and identify their descendants down to $z = 0$. This allows us to measure the actual growth of starforming galaxies. Stellar half-mass sizes and virial radii of these galaxies and their parent halos are plotted in Figure 6.6. For clarity, only galaxies which remain unquenched until $z = 0$ are shown. This has no influence on our results; galaxies which quench at earlier redshifts follow almost identical growth tracks to those which survive until $z = 0$.

Stellar mass and size (left panels) very closely follow virial mass and size (right panels).

Galaxies which form later tend to have lower masses for their size (i.e., lower effective densities), but the rate of size and mass growth is independent of stellar mass. In fact, the most striking aspect of Figure 6.6 is that in these models the relative growth in mass and size of starforming galaxies is very similar, regardless of the stellar mass of these galaxies or the redshift at which they quench. Starforming galaxies grow in size at a rate that is very close to the rate at which their parent halo virial radii increase: $r_{\rm eff} \propto (1+z)^{-1.2}$, and $r_{\rm vir} \propto (1+z)^{-1.3}$. Stellar masses increase slightly faster than virial masses: $M_* \propto (1+z)^{-1.7}$, and $M_{\rm vir} \propto (1+z)^{-1.2}$. Thus, to first order, individual starforming galaxies simply grow in lockstep with their parent halos.

GALAXY SIZES AND QUENCHING

As noted in Section 6.4, the SAMs considered in this paper predict very similar mass-size relations for starforming and quiescent galaxies. This is at odds with observations, especially at $z > 0$ (see Figure 6.4). Observed starforming galaxies are on average a factor $\sim 2-3$ larger than quiescent galaxies at the same stellar mass, while in the models this size difference is on the order of $\sim 10\%$. Apparently galaxy sizes in the models are unaffected by quenching processes. The inclusion of gas dissipation effects during gas-rich mergers (Shankar et al., 2013) does not seem to resolve this problem.

In any case, the lack of size decrease during quenching may have serious consequences for conclusions regarding galaxy structure and galaxy sizes. It implies that no significant structural changes occur during quenching, which is at odds with observed correlations between star formation activity and galaxy structure (e.g., Bell et al. 2012). Relative growth trends should not be strongly affected by this fundamental flaw, but absolute sizes, concentrations, and other parameters should be considered extremely uncertain.

6.5 THE FATE OF QUENCHED GALAXIES

Although the quenching of starforming galaxies contributes significantly to the evolution of the median size of quiescent galaxies, it is very unlikely that quenched galaxies undergo no changes at all. The absence of a significant number of very old, compact galaxies at $z = 0$ means that most, if not all, quiescent galaxies must evolve significantly between $z > 2$ and $z = 0$ (Taylor et al., 2010). We investigate this evolution by selecting galaxies at the moment they quench, and then linking these galaxies to their descendants at lower redshift.

In Figure 6.7 we plot the median evolution in size, virial radius, stellar mass, and virial mass for populations of galaxies quenched at different redshifts. After quenching, "passive" galaxies strongly grow in both size and mass. The rate of stellar mass growth is roughly independent of quenching redshift, although lower-mass galaxies tend to grow slightly more slowly than massive galaxies. Virial mass and size growth are similarly independent of quenching redshift. Galaxy size growth, on the other hand, is slow for recently quenched galaxies, and speeds up as galaxies become older. This results in a negative corre-

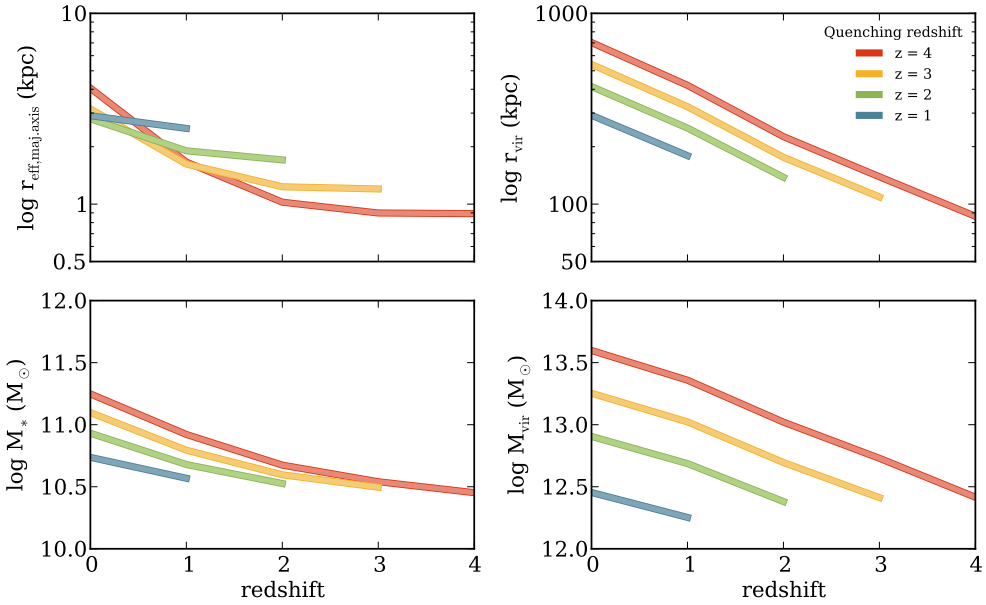

Figure 6.7: Growth in median size, virial radius, stellar mass, and virial mass for galaxies quenched at different redshifts. Both in the Guo and Bower models galaxies grow quite strongly in stellar mass after quenching, at a rate that is mostly independent of quenching redshift. Concurrent with this mass growth, galaxies sizes increase and virial radii and masses increase. At all redshifts older galaxies tend to be more massive and are located in larger halos. This is not the case for galaxy sizes; at high redshift the oldest galaxies tend to be the smallest, while between $z = 0$ and $z = 1$ older galaxies tend to be the largest.

lation between galaxy age and galaxy size at high redshift, which becomes positive between $z = 1$ and $z = 0$.

In order to disentangle the growth in mass and in size, we plot the $z = 0$ mass-size relations for galaxies quenched at different redshifts in Figure 6.8. The solid lines indicate the present-day median mass-size relations for galaxies quenched at different redshifts. At high masses, galaxies of different ages fall onto the same mass-size relation. This same behaviour can be seen at higher redshifts (lower panels). High-mass galaxies undergo a relatively large amount of mergers, which move them onto a common mass-size relation, regardless of when they were quenched. At low masses, however, galaxy growth is dominated by disk instabilities, and mergers play a minor role (e.g., Guo et al. 2011; Shankar et al. 2013). These galaxies therefore tend to remain at the same mass and size after they quench, which results in a clear trend of decreasing size with increasing quenching redshift.

The models analysed in this paper robustly predict that the scatter in age decreases with redshift (at $M_* < 10^{10.5}$). This seems to contradict observations, which show that there is little variation in the scatter up to $z = 2$ (e.g., Newman et al. 2012). However, it is important to realize that observations of the mass-size relation at high redshift are generally

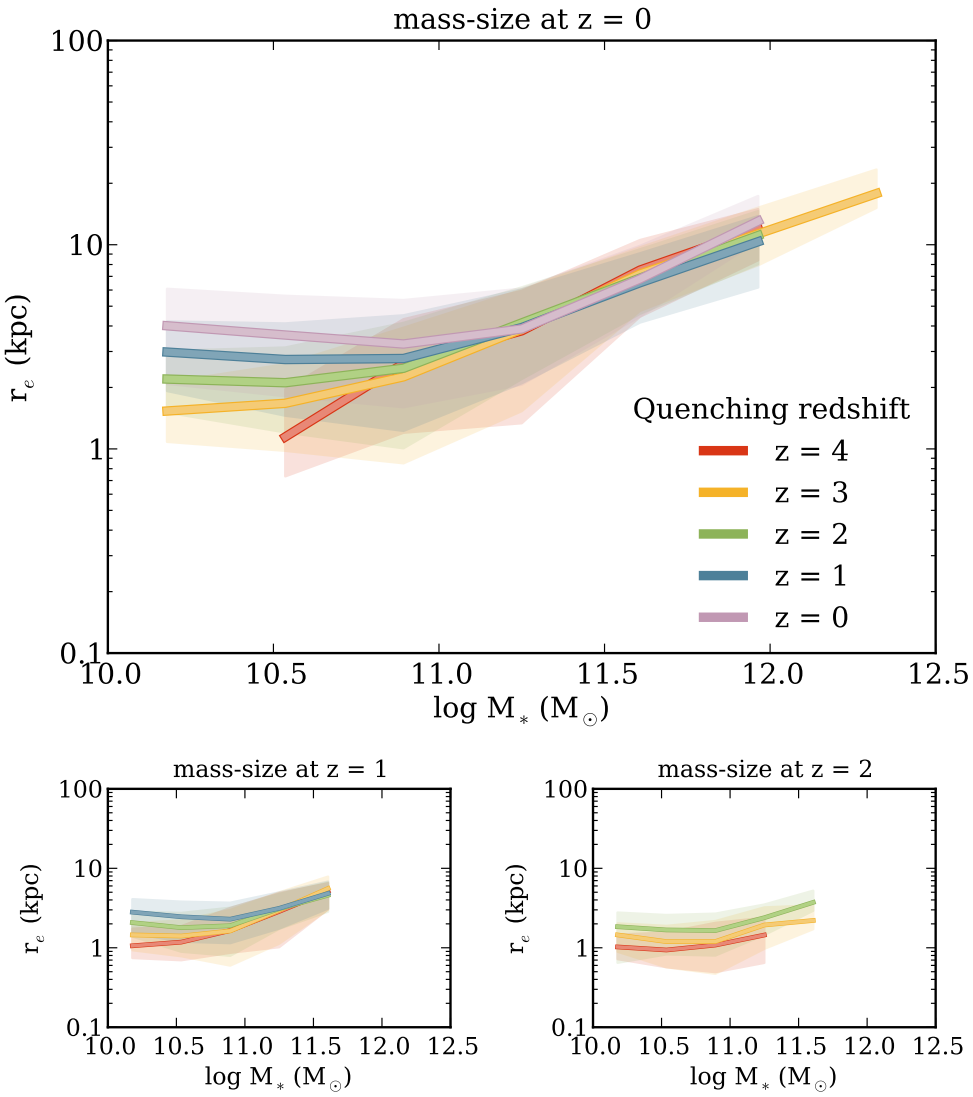

Figure 6.8: Running median of size as a function of stellar mass at $z = 0$ (top panel) and higher redshifts (lower panels) for galaxies quenched at different redshifts. At high masses ($M_* > 10^{11} M_\odot$) galaxies from different epochs lie on a tight mass-size relation. At low masses, however, there is a correlation between quenching redshift and median galaxy size: galaxies which quench early are small compared to galaxies which have quenched late.

only complete down to $M_* \approx 10^{10.5} M_\odot$. Furthermore, power-law fits in the mass-size plane are typically constrained to $M_* > 10^{11} M\odot$. In this region the models predict no changes in the scatter. Galaxy samples with mass limits around $10^{10} M_\odot$ or lower are needed to properly test this prediction.

It should be noted that the SAMs considered in this paper do not include gas dissipation effects during mergers. As shown in Shankar et al. (2013), including such effects results in smaller galaxy sizes for low-mass ($M_* \sim 10^{10} M_\odot$) galaxies. Since gas fractions increase with redshift, the oldest quenched galaxies should be affected more strongly by this effect than more recently quenched galaxies. Therefore, including gas dissipation will only strengthen the age-size trend visible in Figure 6.8, while leaving high-mass galaxies unaffected.

Altough it is obvious from Figure 6.8 that galaxies of different ages have different median sizes at fixed mass, the high number density of galaxies quenched at the lowest redshifts (i.e., the purple and blue lines) may completely wash out this trend in observations. We investigate this in Figure 6.9, by plotting the mean quenching redshift and mass-weighted age in bins of stellar mass and size. Although the age-size correlation is not as obvious as in Figure 6.8, there is clearly a trend. This result is in rough agreement with observations by van der Wel et al. (2009), although the strength of the correlation is weaker in the models, especially at high stellar masses. This may be due to the small size difference between starforming and quiescent galaxies in the models; since the initial spread in sizes of old and newly quenched galaxies is smaller, it takes fewer mergers to wash out the age-size correlation as galaxies move along the mass-size relation.

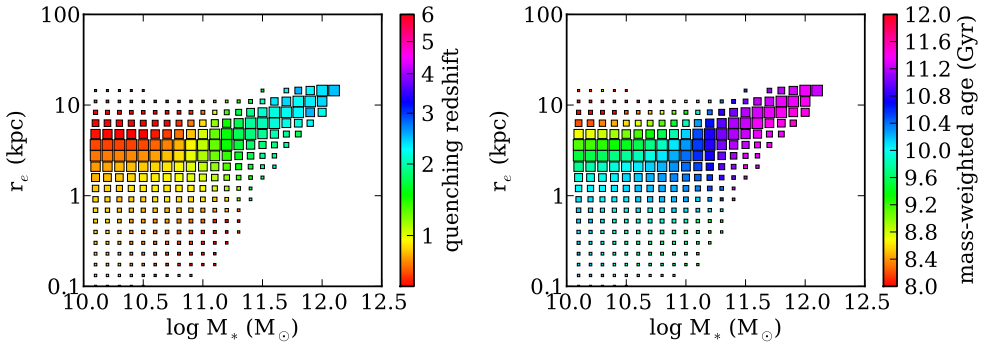

Figure 6.9: Mean quenching redshifts and mass-weighted ages for quiescent galaxies at $z = 0$, as a function of stellar mass and size. High-mass galaxies are on average older and have quenched earlier than low-mass galaxies. At low masses there is a trend between age with size, such that smaller galaxies are on average older than larger galaxies.

6.6 CONCLUSIONS

In this paper we have analysed galaxy size growth as predicted by semi-analytic models. A comparison between different models allows us to identify the aspects of galaxy evolution that are robust to changes in physics implementations, and extract generic predictions regarding galaxy growth. By selecting model galaxies in the same way as is done in observations we can make consistent comparisons between the two. We have compared the growth of model galaxies at fixed mass to recent observations, finding that both SAMs closely match observed quiescent galaxy size growth, despite differences in the exact implementations of disk and bulge assembly. Size growth $\propto (1+z)^{-1}$ seems to be a generic property of these models, driven by the underlying ΛCDM cosmology and very basic assumptions regarding the structure of galaxy bulges and disks.

Starforming galaxies grow at a rate comparable to quiescent galaxies, which can be explained by the fact that recently quenched galaxies dominate the number density of quiescent galaxies at all redshifts. Therefore the bulk of the average size growth of quiescent galaxies is driven by the growth of starforming galaxies. By tracking the growth of populations of starforming galaxies over time we have shown that these galaxies grow almost in lockstep with their parent halos. Thus the size growth of starforming galaxies is very simply tied to the growth of dark matter halos. An important issue is that the size difference between starforming and quiescent galaxies in the models is almost negligible, while in observations this difference is quite large (a factor $\sim 2-4$). This may simply be due to the lack of energy loss due to gas dissipation during gas-rich galaxy mergers, but could also point to severe deficiencies in our understanding of the mechanisms that cause quenching. It is unclear how this issue may be resolved.

Galaxies continue to grow quite rapidly after they quench, increasing in mass and size at a rate comparable to starforming galaxies. The mechanisms by which quiescent galaxies grow depend on galaxy mass. Massive galaxies undergo repeated mergers, which force them onto a tight mass-size relation at $M_* > 10^{11} M_\odot$. At lower masses, quiescent galaxy growth is more strongly driven by disk instabilities instead of mergers. Consequently, low-mass quiescent galaxies tend to remain relatively stationary in the mass-size plane. This results in a strong anticorrelation between galaxy age and galaxy size at $M_* < 10^{11} M_\odot$.

REFERENCES

Bédorf, J., & Portegies Zwart, S. 2013, MNRAS, 431, 767
Bell, E. F., van der Wel, A., Papovich, C., et al. 2012, ApJ, 753, 167
Bower, R. G., Benson, A. J., Malbon, R., et al. 2006, MNRAS, 370, 645
Carollo, C. M., Bschorr, T. J., Renzini, A., et al. 2013, arXiv:1302.5115
Chang, Y.-Y., van der Wel, A., Rix, H.-W., et al. 2013, ApJ, 762, 83
Chang, Y.-Y., van der Wel, A., Rix, H.-W., et al. 2013, arXiv:1305.6931
Cole, S., Lacey, C. G., Baugh, C. M., & Frenk, C. S. 2000, MNRAS, 319, 168
Croton, D. J., Springel, V., White, S. D. M., et al. 2006, MNRAS, 365, 11
Daddi, E., Renzini, A., Pirzkal, N., et al. 2005, ApJ, 626, 680
Dahlen, T., Mobasher, B., Dickinson, M., et al. 2007, ApJ, 654, 172
Damjanov, I., Abraham, R. G., Glazebrook, K., et al. 2011, ApJ, 739, L44
De Lucia, G., & Blaizot, J. 2007, MNRAS, 375, 2
González, J. E., Lacey, C. G., Baugh, C. M., Frenk, C. S., & Benson, A. J. 2009, MNRAS, 397, 1254
Guo, Q., White, S., Boylan-Kolchin, M., et al. 2011, MNRAS, 413, 101
Mo, H. J., Mao, S., & White, S. D. M. 1998, MNRAS, 295, 319
Mo, H. J., Mao, S., & White, S. D. M. 1999, MNRAS, 304, 175
Mosleh, M., Williams, R. J., Franx, M., et al. 2012, ApJ, 756, L12
Naab, T., Johansson, P. H., & Ostriker, J. P. 2009, ApJ, 699, L178
Nagy, S. R., Law, D. R., Shapley, A. E., & Steidel, C. C. 2011, ApJ, 735, L19
Newman, A. B., Ellis, R. S., Bundy, K., & Treu, T. 2012, ApJ, 746, 162
Oogi, T., & Habe, A. 2013, MNRAS, 428, 641
Oser, L., Ostriker, J. P., Naab, T., Johansson, P. H., & Burkert, A. 2010, ApJ, 725, 2312
Oser, L., Naab, T., Ostriker, J. P., & Johansson, P. H. 2012, ApJ, 744, 63
Patel, S. G., van Dokkum, P. G., Franx, M., et al. 2013, ApJ, 766, 15
Sérsic, J. L. 1968, Atlas de galaxias australes (Cordoba, Argentina: Observatorio Astronomico, 1968)
Shankar, F., Marulli, F., Bernardi, M., et al. 2010, MNRAS, 403, 117
Shankar, F., Marulli, F., Bernardi, M., et al. 2010, MNRAS, 405, 948
Shankar, F., Marulli, F., Bernardi, M., et al. 2013, MNRAS, 428, 109
Shen, S., Mo, H. J., White, S. D. M., et al. 2003, MNRAS, 343, 978
Somerville, R. S., Barden, M., Rix, H.-W., et al. 2008, ApJ, 672, 776
Springel, V., White, S. D. M., Jenkins, A., et al. 2005, Nature, 435, 629
Szomoru, D., Franx, M., Bouwens, R. J., et al. 2011, ApJ, 735, L22
Szomoru, D., Franx, M., van Dokkum, P. G., et al. 2013, ApJ, 763, 73
Taylor, E. N., Franx, M., Glazebrook, K., et al. 2010, ApJ, 720, 723
Toft, S., van Dokkum, P., Franx, M., et al. 2007, ApJ, 671, 285
Trujillo, I., Förster Schreiber, N. M., Rudnick, G., et al. 2006, ApJ, 650, 18
Trujillo, I., Feulner, G., Goranova, Y., et al. 2006, MNRAS, 373, L36
van der Wel, A., Bell, E. F., van den Bosch, F. C., Gallazzi, A., & Rix, H.-W. 2009, ApJ,

698, 1232
van der Wel, A., Rix, H.-W., Wuyts, S., et al. 2011, ApJ, 730, 38
van Dokkum, P. G., Franx, M., Kriek, M., et al. 2008, ApJ, 677, L5
Williams, R. J., Quadri, R. F., Franx, M., van Dokkum, P., & Labbé, I. 2009, ApJ, 691, 1879
Williams, R. J., Quadri, R. F., Franx, M., et al. 2010, ApJ, 713, 738
Williams, R. J., Quadri, R. F., & Franx, M. 2011, ApJ, 738, L25